

# A prospective, randomized, placebo-controlled, double-blinded, and split-face clinical study on LED phototherapy for skin rejuvenation: Clinical, profilometric, histologic, ultrastructural, and biochemical evaluations and comparison of three different treatment settings

Seung Yoon Lee<sup>a,\*</sup>, Ki-Ho Park<sup>b</sup>, Jung-Woo Choi<sup>c</sup>, Jung-Kyun Kwon<sup>d</sup>,  
Doo Rak Lee<sup>a</sup>, Mi Sun Shin<sup>a</sup>, Jee Sung Lee<sup>e</sup>, Chung Eui You<sup>a</sup>, Mi Youn Park<sup>a</sup>

<sup>a</sup> Department of Dermatology, National Medical Center, 18-79, Euljiro 6-ga, Jung-ku, Seoul, Republic of Korea

<sup>b</sup> Quantitative Real-Time PCR Lab, Clinical Research Institute, Seoul National University Hospital, 28, Yeongun-dong, Jongno-ku, Seoul, Republic of Korea

<sup>c</sup> Department of Pathology, Korea University Hospital, 126-1, Anam-dong 5-ga, Seongbuk-ku, Seoul, Republic of Korea

<sup>d</sup> Department of Electron Microscope Laboratory, College of Medicine, Hanyang University, 17, Haengdang-dong, Seongdong-ku, Seoul, Republic of Korea

<sup>e</sup> Division of Biostatistics, Graduate School of Public Health, Korea University, 126-1, Anam-dong 5-ga, Seongbuk-ku, Seoul, Republic of Korea

Received 8 January 2007; received in revised form 10 April 2007; accepted 11 April 2007

Available online 1 May 2007

## Abstract

Light-emitting diodes (LEDs) are considered to be effective in skin rejuvenation. We investigated the clinical efficacy of LED phototherapy for skin rejuvenation through the comparison with three different treatment parameters and a control, and also examined the LED-induced histological, ultrastructural, and biochemical changes. Seventy-six patients with facial wrinkles were treated with quasi-monochromatic LED devices on the right half of their faces. All subjects were randomly divided into four groups treated with either 830 nm alone, 633 nm alone, a combination of 830 and 633 nm, or a sham treatment light, twice a week for four weeks. Serial photography, profilometry, and objective measurements of the skin elasticity and melanin were performed during the treatment period with a three-month follow-up period. The subject's and investigator's assessments were double-blinded. Skin specimens were evaluated for the histologic and ultrastructural changes, alteration in the status of matrix metalloproteinases (MMPs) and their tissue inhibitors (TIMPs), and the changes in the mRNA levels of IL-1 $\beta$ , TNF- $\alpha$ , ICAM-1, IL-6 and connexin 43 (Cx43), by utilizing specific stains, TEM, immunohistochemistry, and real-time RT-PCR, respectively. In the results, objectively measured data showed significant reductions of wrinkles (maximum: 36%) and increases of skin elasticity (maximum: 19%) compared to baseline on the treated face in the three treatment groups. Histologically, a marked increase in the amount of collagen and elastic fibers in all treatment groups was observed. Ultrastructural examination demonstrated highly activated fibroblasts, surrounded by abundant elastic and collagen fibers. Immunohistochemistry showed an increase of TIMP-1 and 2. RT-PCR results showed the mRNA levels of IL-1 $\beta$ , TNF- $\alpha$ , ICAM-1, and Cx43 increased after LED phototherapy whereas that of IL-6 decreased. This therapy was well-tolerated by all patients with no adverse effects. We concluded that 830 and 633 nm LED phototherapy is an effective approach for skin rejuvenation.

© 2007 Elsevier B.V. All rights reserved.

**Keywords:** Light-emitting diodes; Light therapy; Phototherapy; Photorejuvenation; Skin rejuvenation; Non-ablative rejuvenation

## 1. Introduction

Aging skin presents various unpleasant-looking morphologic changes such as wrinkles, dyspigmentation, telan-

\* Corresponding author. Tel.: +82 2 2260 7315; fax: +82 2 2277 0915.  
E-mail address: [drly96@hotmail.com](mailto:drly96@hotmail.com) (S.Y. Lee).

giectasia, and loss of elasticity. Both chronological and environmental influences are involved in the aging process of the skin, among which photodamage is one of the most important components [1,2]. Several characteristic histological features are observed in photodamaged skin, for example, reduction in the amount of collagen, fragmentation of collagen fibers, elastotic degeneration of elastic fibers, dilated and tortuous dermal vessels, and atrophy and disorientation of the epidermis [3,4].

So far, various rejuvenation modalities have attempted to reverse the dermal and epidermal signs of photo- and chronological aging. At the center of these treatments have been ablative methods which remove the epidermis and induce a controlled form of skin wounding to promote collagen biosynthesis and dermal matrix remodeling, such as dermabrasion, chemical peels, and ablative laser resurfacing with carbon dioxide (CO<sub>2</sub>) or erbium: yttrium-aluminum-garnet (Er:YAG) lasers or a combination of these wavelengths [5–7]. However, these procedures require intensive post-treatment care with frequent changing of dressings, and more importantly, can lead to considerable complications including long-lasting erythema, pain, infection, bleedings, oozing, hyper- or hypopigmentation and sometimes scarring [8,9]. Patient dissatisfaction with the prolonged downtime and the clinician's desire for safer and effective rejuvenation with fewer side effects drove investigations into the development of novel skin rejuvenation procedures, leading to the appearance in the skin rejuvenation armamentarium of various nonablative rejuvenation technologies [10,11].

Nonablative skin rejuvenation aims to improve photo-aged skin without destroying the epidermis [10–12]. It has been arbitrarily classified into two types, that is, type I and type II photorejuvenation [12]. The former primarily targets irregular pigmentation and telangiectasia and includes intense pulsed light (IPL) sources, 532 nm potassium-titanyl-phosphate (KTP) lasers, and high-dose 585/595 nm pulsed dye lasers (PDL), while the latter aims for wrinkle reduction and skin tightening and utilizes amongst other photothermal modalities IPL systems [13–15], low-dose 585 nm PDLs [16–21], 1064 & 1320 nm neodymium: yttrium-aluminum-garnet (Nd:YAG) lasers [22], 1450 nm diode lasers [23], and 1 540 nm erbium glass lasers [24].

The light-emitting diode (LED) is a novel light source for nonablative skin rejuvenation. It is considered to be effective for improving wrinkles and skin laxity, thus being classified under type II photorejuvenation [12,25–29]. Whereas most other techniques for type II photorejuvenation use heat energy to cause controlled thermal injury to the dermis (photothermolysis) [10–24], LED phototherapy is a non-thermal and atraumatic treatment which stimulates cell activities and functions through a photobiomodulative effect. Photobiomodulation is the process where the incident photons are absorbed by chromophores, for example in the respiratory chain of the mitochondria for longer wavelength visible light and in cellular membranes for near infrared light, to modulate various cell functions and is

believed to result in new collagen synthesis to exert the effects leading to rejuvenation [25–36]. However, there is a lack of well-designed clinical studies performed in a randomized, controlled trial using objective methods to measure the treatment efficacy [12]. In the present study, we performed a prospective, randomized, placebo-controlled, double-blinded, and split-face clinical trial to determine the clinical efficacy of LED phototherapy for skin rejuvenation, and investigated post-phototherapy histological, ultrastructural, and biochemical changes. The clinical efficacy was assessed objectively by using profilometry and other instrumental measurements of the skin elasticity and amount of melanin. In addition, three treatment settings with different wavelengths of LEDs were compared in regards to the clinical, histologic, ultrastructural and biochemical changes after treatment.

## 2. Materials and methods

### 2.1. Patients

A total of 112 patients (2 males and 110 females), ranging in age from 35 to 55, with visible signs of aging were recruited for this study and randomly divided into four groups of 28 patients each. The number of subjects was calculated statistically (SAS version 9.1), so that this study would detect differences in the mean percentage improvements among the four different treatment groups when the maximum standardized effect size was larger than 0.5, at a 5% significance level, using an analysis of variance (ANOVA) with 80% power, allowing 10% extra for drop-outs [37]. Exclusion criteria included a history of photosensitivity or recent use of photosensitizing drugs including systemic retinoids, recent use of topical retinoic acid, recent history of any skin disease, operation, trauma, systemic disease that could affect the skin status, psychological disease, pregnancy, lactation and smoking. Patients were also excluded if they had had any other previous aesthetic procedures, such as botulinum toxin (botox) or filler injection, laser resurfacing, chemical peels, dermabrasion, or nonablative rejuvenation treatments, within the three years previous to the trial. This study was approved by our institutional review board. Written informed consent for the treatment and for the clinical photography was obtained from all study patients. Nineteen patients who volunteered to undergo biopsies gave their signed consent forms before entry to the trial.

### 2.2. Light source

The phototherapy system used as the light source for this study consisted of a base and interchangeable heads emitting quasimonochromatic light of each different preset wavelength from adjustable planar arrays of LEDs. The near infrared head (Omnilux plus<sup>TM</sup>, Photo Therapeutics Ltd., Fazeley, UK) comprised five articulated panels containing 108 LEDs each, so that they could be adjusted to

fit the contour of the patient's face optimally. The red light head (Omnilux revive<sup>TM</sup>, Photo Therapeutics Ltd.) consisted of four panels containing 420 LEDs each arranged in the same way. The treatment heads delivered symmetrical peak wavelengths;  $830 \pm 5$  nm for the infrared light and  $633 \pm 6$  nm for the red light. The irradiance was  $55$  mW/cm<sup>2</sup> for the infrared light and  $105$  mW/cm<sup>2</sup> for the red light at a distance of 1 to 10 centimeters from the light source. The radiant fluences, or doses, during a single treatment for twenty minutes were  $66$  J/cm<sup>2</sup> and  $126$  J/cm<sup>2</sup> for the infrared and red treatment heads, respectively.

### 2.3. Study design

All patients were randomly divided using computer-generated random numbers into four groups of 28 patients each. Group 1 was treated with the 830 nm head alone, group 2 with the 633 nm head alone, group 3 with a combination of the 830 and 633 nm heads by alternating them in that order, and group 4 with a sham treatment light as the control group. We used the standby mode of the 633 nm LED head as the sham treatment.

In all groups, the patients were treated only on the right half of the face with the left half being occluded. The split-face model within the control group was set to detect any possible effects of the sham treatment. This study design allowed us two ways to compare the clinical efficacy; a within-patient comparison between the treated right side and the covered left side, and a group-to-group comparison between the treated sides of three treatment groups and those of the control group, which offered a tool of double-checking the differences. The use of objective methodology which offered numerical values representing the clinical efficacy technically enabled this 'double comparison'.

Objective instrumental measurements of the melanin level and the skin elasticity were carried out before treatment; at every treatment session for the former, at every other treatment session for the latter. After the measurements, each patient washed his/her face and was treated for twenty minutes in the supine position with the wavelength of light as set by the protocol of his/her group. The distance between the irradiating head and the patient's nose was about 3–5 cm. In group 3, we alternated sessions of the 830 nm and 633 nm LED treatment in succession, with the 830 nm treatment head being used first. Goggles were worn to protect the retinae from direct illumination. When the treatment was over, the instrumental measurements for the melanin level were performed in the same way as before treatment. In this manner, the therapy was performed twice a week for four weeks at a three to four-day interval between each session.

### 2.4. Clinical assessment

Digital clinical photography (Canon 300 D) of both periorbital areas of each patient was taken at baseline, at week 3 during the treatment period, and at 2, 4, 8, and 12 weeks

after the treatment completion. Profilometric evaluation using silicon imprints (Visiometer SV600<sup>TM</sup>, Courage+Khazaka, Köln, Germany) was performed on the outer canthus of both periorbital areas (so-called crow's feet zone) at baseline and at 2, 4, 8, and 12 weeks after the final treatment session. Objective instrumental measurements of the melanin level were carried out with a Mexameter<sup>TM</sup> (Courage+Khazaka) before and after each treatment session, and measurements of the skin elasticity were performed with a Cutometer<sup>TM</sup> (Courage+Khazaka) at baseline, at weeks 2, 3 and 4 during the treatment period, and at 2, 4, 8, and 12 weeks after the final treatment session. The sites of evaluation were identical for a given measurement through all assessment points. All measurements were performed by the same physician.

### 2.5. The subject and the investigator global assessments

The subjects were kept unaware as to which group they had been randomly assigned throughout the study period. The subject global assessment, or satisfaction level, was evaluated at week 3 during the treatment period and at 2, 4, 8, and 12 weeks after the treatment completion by rating on a six-point scale (worse, no change, fair, good, and excellent) by the patients themselves.

The investigator's assessment was performed by two blinded dermatologists through evaluation of the serial clinical photos with random codes. Their assessment was rated on a five-point scale and scored as follows; –1 for worse, 0 for no change, 1 for mild improvement, 2 for moderate improvement, and 3 for marked improvement. The results of the assessment were gathered and analyzed retaining the random coding. The codes were broken only after the assessments were finished.

### 2.6. Tissue assay evaluation

#### 2.6.1. Preparation of the specimens

A total of 19 patients volunteered for punch biopsies; 5 in group 1, 6 in group 2, 5 in group 3, and 3 in group 4. From among them, two patients randomly chosen for each group had 3 mm punch biopsies on the extensor surface of their left forearms before the first treatment and 20 minutes after the last treatment. In these patients, their left forearm received real or sham treatment identical to that delivered to their face. The specimens from these patients were processed for real time reverse transcriptase-polymerase chain reaction (RT-PCR) to measure the messenger ribonucleic acid (mRNA) levels of interleukin-1 $\beta$  (IL-1 $\beta$ ), tumor necrosis factor- $\alpha$  (TNF- $\alpha$ ), interleukin-6 (IL-6), intercellular adhesion molecule-1 (ICAM-1), and connexin-43 (Cx43).

The remaining volunteers from each group had 2 mm punch biopsies on the lateral aspect of their right cheeks before the first treatment and 2 weeks after the last treatment. The specimens taken before the first treatment from these patients were embedded in paraffin and processed for

histologic examination with hematoxylin and eosin (H & E) stain, Verhoeff-van Gieson stain, Alcian blue stain (pH 2.5), Schmorl's stain, and immunohistochemistry. Those taken at two weeks after the final treatment were split vertically into two pieces; one undergoing the same examination as before treatment, and the other being processed for transmission electromicroscopy (TEM). Any given procedure was performed at the same time by the same technician only after all pre- and post-treatment specimens were gathered to avoid any possible biases.

### 2.6.2. Transmission electromicroscopy

The skin specimens were fixed at 4 °C for 3 hours in cold-buffered 2.5% glutaraldehyde in phosphate buffered saline (PBS, pH 7.4) and then post fixed at 4 °C for 1 hour and 30 minutes in 1% osmium tetroxide. After gradual dehydration in an ascending ethanol series, the tissues were transferred into propylene oxide, embedded with an Epon Embedding kit (Ted Pella, Inc. CA, USA) and polymerized at 60 °C for 72 hours in a TD-500 Electron Microscope oven (DOSAKA EM CO. Ltd., Kyoto, Japan). Tissue blocks were trimmed into both thick sections (1 μm) which were stained with 1% toluidine blue for light microscopy and thin sections (80 nm) which were double stained with uranyl acetate and lead citrate. The sections were sliced with a Reichert-Jung Ultracut E ultramicrotome (Leica Microsystems, Wetzlar, Germany). All of the thin sections were examined with an H-7600s transmission electron microscope (Hitachi, Tokyo, Japan), 80 kV acceleration voltage.

### 2.6.3. Immunohistochemical staining

Immunohistochemical staining was performed using a peroxide technique. Formalin-fixed paraffin-embedded tissue blocks were sectioned to a thickness of 4 μm. Sections were deparaffinized for 5 minutes three times in xylene and rehydrated for 5 minutes per session in serial-graded alcohol (100%, 95%, 80%, 70% alcohol). Antigen retrieval was performed for MMP-1 and TIMP-2. For antigen retrieval, 10 mM citrate buffer (pH 6.0) was heated in a pressure cooker for 10 minutes. After that, the container was cooled for 20 minutes at room temperature. Endogenous peroxide activity was blocked by 3% hydrogen peroxide in methanol for 10 minutes. The slides were washed three times in Tris-buffered saline (TBS, pH 7.6) for 5 minutes and incubated with a blocking solution (normal goat serum) at room temperature for 20 minutes.

The antibodies then used were as follows: an anti-MMP-1 antibody (dilution titer 1:200, Lab Vision, California, USA); an anti-MMP-2 antibody (dilution titer 1:50, Lab Vision); an anti-TIMP-1 antibody (dilution titer 1:100, Lab Vision); and an anti-TIMP-2 antibody (dilution titer 1:50, Lab Vision). The antibodies were incubated for 30 minutes at room temperature and washed three times in TBS for 5 minutes. Subsequently, secondary antibody reaction was achieved with a ChemMate DAKO EnVision Detection Kit (Dako, Denmark) for about 30 minutes at room temperature. After washing with TBS, the samples were stained with 3,3'-diaminobenzidine for chromogenic reaction and counter-stained with hematoxylin for 30 seconds.

### 2.6.4. Real time RT-PCR

Total RNA was extracted from skin samples with a Trizol kit (Invitrogen Corp., Carlsbad, California). Reverse transcription was performed using 1.5 μg of total RNA in 20 μL using a Reverse Transcription Kit (Invitrogen). For real-time PCR assays, a master mix of the following components was prepared, at the indicated final concentrations: 2.5 μL each primer (9 μM), 2.5 μL probe (2.5 μM), 2.5 μL water, and 12.5 μL TaqMan PCR 2X master mixture (Applied Biosystems, Lincoln, CA). The PCR primers and probes used are listed in Table 1. Five microliters of reverse transcription reaction mixture was added as a PCR template. Relative quantitative real-time PCR was performed using the above reagents using an ABI Prism 7000 Sequence Detection System (Perkin-Elmer Applied Biosystems, Lincoln, CA). The following procedure was used. After initial activation of uracyl-N-glycosylase at 50 °C for 2 minutes, AmpliTaq Gold (Applied Biosystems) was activated at 95 °C for 10 minutes. PCR consisted of 45 amplification cycles (denaturation at 95 °C for 15 seconds, annealing at 60 °C for 1 minute, and extension at 60 °C for 1 minute). During PCR amplification, the amplified product amount was monitored by continuous measurement of fluorescence. The expression of the genes was normalized versus a GAPDH (VIC/MGB probe, primer limited) as follows; the cycle number at which the transcripts of the genes were detectable (threshold cycle, Ct) was normalized against the Ct of GAPDH, which is referred to as delta Ct. The expression of the genes relative to a reference was expressed as  $2^{-\text{deltadeltaCt}}$ , where  $\text{deltadeltaCt}$  refers to the difference in the values of deltaCt between the test groups and the reference.

Table 1  
Sequences of the probes and primers for real time RT-PCR

	Assay ID	Sequence
IL-1β	Hs00174097_m1	5'-GGAGCAACAAGTGGTGTCTCCATG-3'
TNF-α	Hs00174128_m1	5'-CCCATGTTGTAGCAAACCCTCAAGC-3'
IL-6	Hs00174131_m1	5'-TTCAATGAGGAGACTTGCTGGTGA-3'
ICAM-1	Hs00164932_m1	5'-TCCTCACCGTGTACTGGACTCCAGA-3'
Connexin 43	Hs00748445_s1	5'-GACCAGTGGTGCCTGAGCCCTGCC-3'

## 2.7. Statistical analysis

Repeated measures of analysis of variance (RM-ANOVA) were used to evaluate the significance of the changes in the R3 values of the Visiometer<sup>TM</sup> and in the R2 values of the Cutometer<sup>TM</sup>, between baseline and subsequent assessments in each treated side and covered side within a same individual, and also between the treated sides of the three treatment groups and those of the control group. The differences in the melanin levels between before and after each treatment were analyzed using sign rank tests with the medians.

## 3. Results

### 3.1. Patient characteristics

Seventy six (1 male and 75 females) out of 112 patients completed the whole study protocol. Ten subjects were skin type III and 66 were type IV. Dropout of the subjects occurred mostly due to a schedule conflict, follow-up loss, or dissatisfaction with the treatment. Their data were excluded from the final analysis. The demographic data of the patients, described in Table 2, were not statistically different among the four groups.

### 3.2. Clinical efficacy

#### 3.2.1. Severity of wrinkles

The R3 value, which refers to the average roughness, was chosen for the analysis, because it is the most representative parameter to show wrinkle severity. As the wrinkle severity increases, the R3 value also increases. The statistical analysis revealed a significant decrease in R3 values on the treated sides of the patients in group 1, group 2, and group 3, according to time passed from the baseline. On the other hand, no noticeable change was found on the exposed sides

in group 4 (the control group) (Fig. 1a). On the covered sides, no significant serial differences between before and after treatment were observed in all four groups (Fig. 1b).

The p-values for ANOVA indicated statistically significant differences in the double comparison of wrinkle reduction; both between the treated and covered side within the same individual of the treatment groups (Fig. 1b), and between the exposed sides of the treatment groups and those of the control group (Fig. 1a, representing mean percentage reduction), at any subsequent assessment time point, while it was not achieved in the control group. The maximum mean percentage improvement of the average roughness, when compared to baseline, was 36%, which was achieved in group 3 (830 nm and 633 nm) at 3 months after treatment completion. The final mean percentage improvements in groups 1 (830 nm alone) and 2 (633 nm alone) were 33% and 26%, respectively. Improvements in the severity of wrinkles in the treatment groups were clearly observed on the clinical photos as well (Fig. 1c).

#### 3.2.2. Skin elasticity

The R2 value, which refers to the gross elasticity, was used for the analysis. It represents the ability of reformation of the skin and is the most important parameter to indicate the skin elasticity. The nearer the value gets towards 1, the better is the skin elasticity.

The statistical analysis showed a significant increase in R2 values on the treated sides in group 1, group 2, and group 3, according to time passed from the baseline, whereas no significant serial change was found on the exposed sides in group 4 (the control group) (Fig. 2a). We could not observe any significant serial difference between before and after treatment on the covered sides in all four groups (Fig. 2b).

The p-values for ANOVA revealed statistically significant differences in the double comparison of skin elasticity (Fig. 2). The maximum mean percentage increase of the R2 value was 19%, which was observed in group 1 at 3 months after treatment completion. The final increase rates in groups 2 and 3 were 14% and 16%, respectively.

#### 3.2.3. Melanin level

Only the data of group 2 showed a statistically significant decrease in the melanin levels after treatment compared to before treatment (Table 3). The mean of the differences was  $-14.61 \pm 7.15$  on the treated sides in group 2, while it was  $-1.84 \pm 7.59$  in the covered sides in the same group. There was no statistically significant difference between before and after treatment both on exposed sides and covered sides in the other treatment groups or the control group, although a varied tendency was observed for the melanin levels to decrease slightly.

### 3.3. The subject and the investigator global assessments

The subjects' satisfaction levels between the treatment groups and the control group were clearly contrasted, as

Table 2  
Demographic data of the subjects of each group and reasons of dropouts

Group	Number of patients	Age (Mean $\pm$ Std)	p-value	Reasons for dropout
Group 1 (830 nm alone)	21	48.10 $\pm$ 5.80	0.3857	4: schedule conflict 3: follow-up loss
Group 2 (633 nm alone)	18	47.78 $\pm$ 6.43		3: schedule conflict 5: follow-up loss 1: admission due to other disease 1: move to other region
Group 3 (830 nm and 633 nm)	22	46.91 $\pm$ 4.08		3: schedule conflict 3: follow-up loss
Group 4 (Control sham light)	15	45.07 $\pm$ 5.48		10: dissatisfaction with the treatment 2: schedule conflict 1: follow-up loss

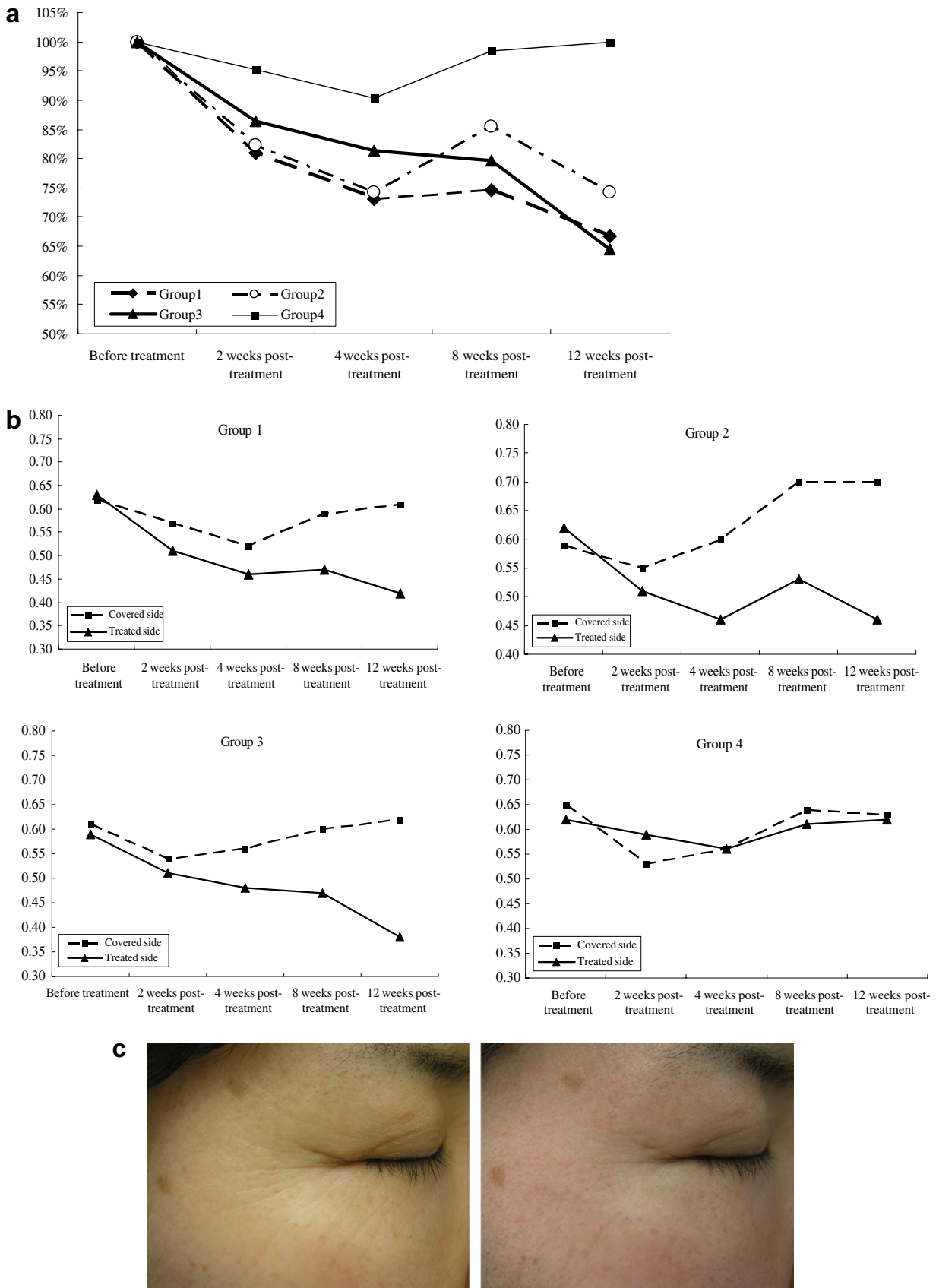
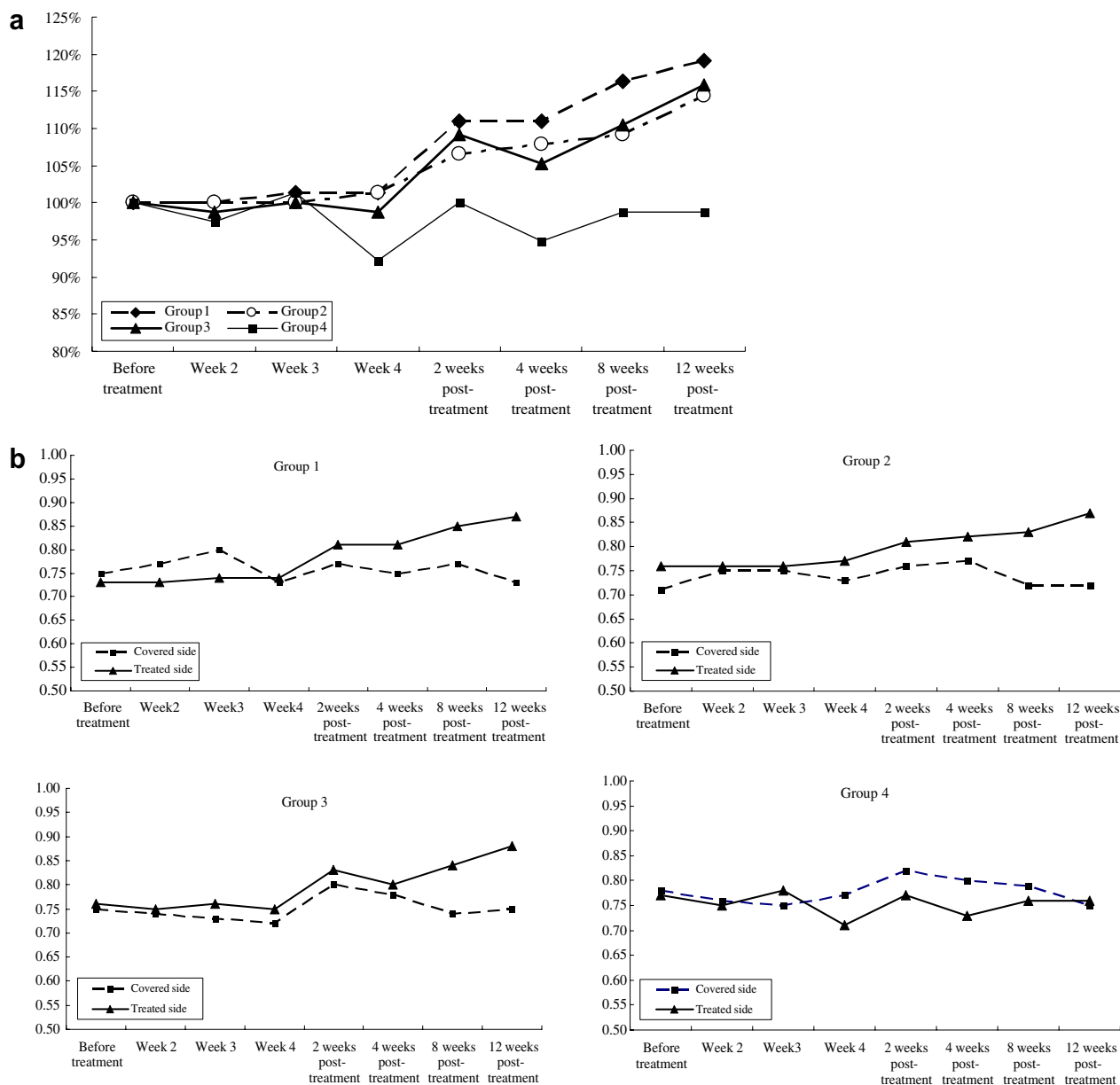


Fig. 1. The severity of wrinkles (represented as average roughness, R3 value) decreased significantly in the treated sides of the treatment groups compared to baseline, which was not observed in the covered sides of all groups or in the treated sides of the control group. (a) Percentage reduction of R3 values (average roughness) in the treated sides of each group. (b) Comparison of R3 values between the treated sides and the covered sides within each group. (c) Clinical photos showing an improvement of periorbital wrinkles 3 months after LED phototherapy (right) compared to the baseline (left).



**Fig. 2.** The elasticity of the skin (represented as net elasticity, R2 value) increased significantly in the treated sides of the treatment groups, which was not observed in the covered sides of all groups or in the treated sides of the control group. (a) Percentage increase of R2 values (net elasticity) in the treated sides of each group. (b) Comparison of R2 values between the treated sides and the covered sides within each group.

shown by the high proportion of 'good' and 'excellent' in the three treatment groups versus the majority occupied by 'no change' in the control group (Fig. 3). A tendency for the satisfaction levels to get noticeably higher over time was noted, beginning 4 weeks after treatment completion. At the final assessment, group 1 (830 nm alone) and group 3 (830 nm and 633 nm) showed the greatest proportion of highly satisfied patients (those who answered as 'good' or 'excellent'), of 95.2% (20 out of 21) and 95.5% (21 out of 22), respectively, which was considerably higher than that of group 2 (72.3%, 13 out of 18). In the control group, it was 13.3% at the last follow-up point.

There was a particular case where a 55-year-old woman, who was included in group 1, expressed great satisfaction with a marked improvement of telangiectasia on her cheeks (Fig. 4), the mechanism for which remains speculative. No adverse effect was reported during the whole study period.

The investigators' global assessment is shown in Table 4. The score indicating the degree of improvement in wrinkle severity was higher in the treated sides of groups 1, 2, and 3 than in group 4. The average scores in the treatment groups were over 2, which indicated that there was more than 'moderate improvement' in these groups. However, in the control group, the scores were below 0.5 in both treated

Table 3

The melanin levels decreased to a statistically significant level after 633 nm alone treatment (Group 2), whereas the changes were not significant in other groups in spite of a tendency of slight decrease in the melanin levels

Group		Differences		
		Mean $\pm$ std	Median	p-value <sup>a</sup>
Group 1 (830 nm alone)	Covered	-5.43 $\pm$ 6.86	-7.05	0.4663
	Treated	-6.94 $\pm$ 7.66	-8.95	
Group 2 (633 nm alone)	Covered	-1.84 $\pm$ 7.59	-1.89	<0.0001 <sup>b</sup>
	Treated	-14.61 $\pm$ 7.15	-15.47	
Group 3 (830 nm and 633 nm)	Covered	-6.27 $\pm$ 5.92	-5.94	0.0955
	Treated	-9.74 $\pm$ 6.68	-11.34	
Group 4 (Control sham light)	Covered	-3.38 $\pm$ 6.87	-4.16	0.241
	Treated	-1.03 $\pm$ 5.24	0.84	

<sup>a</sup> P-values are for paired *t*-test.

<sup>b</sup> Statistically significant.

and covered sides, which meant that there was no noticeable improvement in this group.

### 3.4. Results from tissue assays

#### 3.4.1. Collagen fibers

On standard preparation with H & E, a significant increase in the amount of collagen fibers was observed at 2 weeks post-treatment in the treatment groups (Fig. 5a). This finding was confirmed by Masson-trichrome stains (Fig. 5b). The increase of collagen was observed through the entire dermis, the most significantly changed parts of which were the perifollicular areas and the papillary and upper reticular dermis in which a clearly visible Grenz zone was created, displacing the previously degenerated dermal matrix. In addition, the arrangement of collagen bundles

was more packed and well-organized and the thickness of each bundle appeared greater than before treatment. On the other hand, in the control group, we could not observe any noticeable increase in the amount of collagen on the H& E preparation, although a slight increase of collagen fibers in the superficial layer of the upper reticular dermis was recognized with the Masson-trichrome stain. No significant change was found in regards to the epidermis in either the treatment or the control groups.

#### 3.4.2. Elastic fibers

Evaluation of the specimens with Verhoeff-van Gieson stains demonstrated a significant increase of the amount of elastic fibers in the upper to mid-reticular dermis at 2 weeks post-treatment in the treatment groups (Fig. 6). Alcian blue staining was performed to determine whether these increased elastic fibers were normal or elastotically degenerated. Elastotic material is stained blue with Alcian blue stain, because it characteristically contains a large amount of acid mucopolysaccharides. The results were negative in the areas where increased elastic fibers were observed in all treatment groups, which suggested that they were normal elastic fibers and not elastotic material. On the other hand, elastic fibers did not increase in the control group, so Alcian blue staining was not performed.

#### 3.4.3. Ultrastructural findings

In the TEM examination, the most notable finding was the presence of highly activated fibroblasts in the treatment groups and the increased size and number of collagen and elastic fibers. The fibroblasts appeared enlarged and presented numerous dilated endoplasmic reticula, surrounded by abundant thick collagen bundles and normal-structured

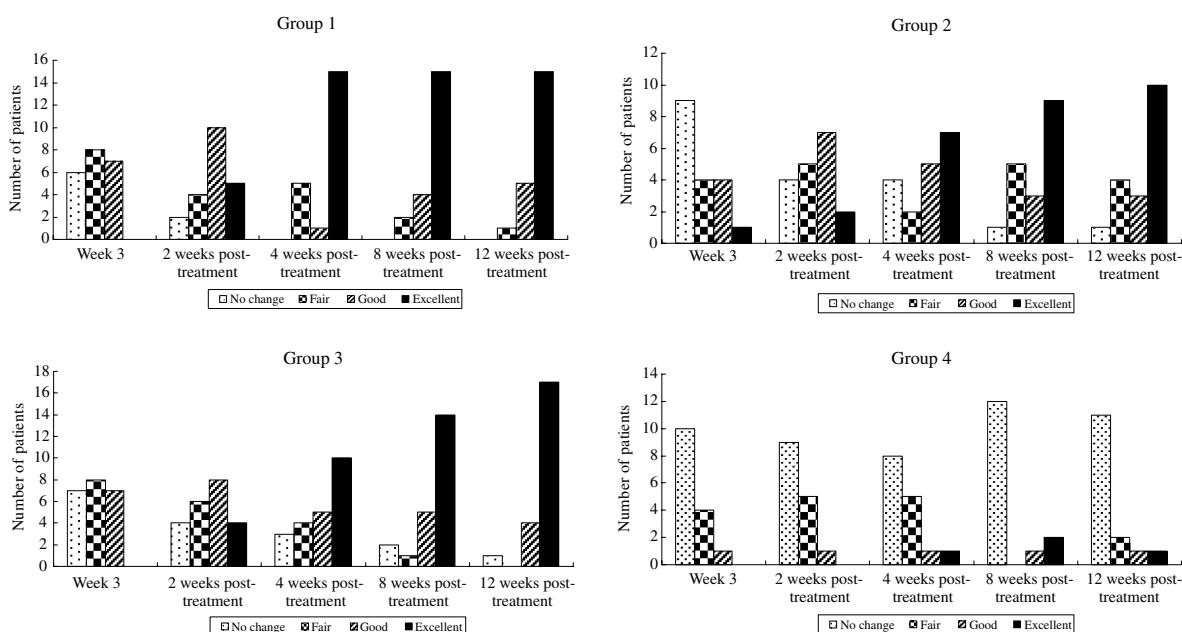


Fig. 3. The subjects' assessment showed that the satisfaction levels with the treatment were significantly higher in the treatment groups than in the control group.

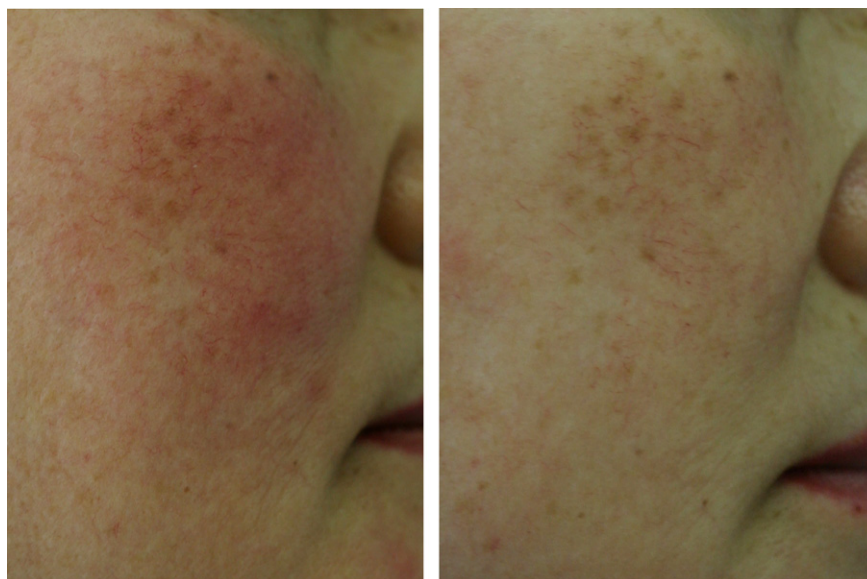


Fig. 4. A marked improvement of telangiectasia was observed in a 55-year-old woman, who had been treated with 830 nm alone (Left: before treatment, Right: 3 months after treatment completion).

Table 4  
Investigators' assessment of improvement in the severity of wrinkles

	Group 1 (830 nm alone)		Group 2 (633 nm alone)		Group 3 (830 nm and 633 nm)		Group 4 (Control sham light)	
	Treated	Covered	Treated	Covered	Treated	Covered	Treated	Covered
Assessor 1	2.38 ± 0.65	0.29 ± 0.63	2.06 ± 0.78	0.33 ± 0.75	2.41 ± 0.72	0.32 ± 0.82	0.33 ± 0.70	0.20 ± 0.65
Assessor 2	2.57 ± 0.66	0.14 ± 0.64	2.17 ± 0.76	0.28 ± 0.65	2.45 ± 0.66	0.36 ± 0.71	0.13 ± 0.62	0.07 ± 0.57

elastic fibers (Fig. 7). On the other hand, in the control group, the fibroblasts were normal in size and spindle-shaped and did not have dilated or increased endoplasmic reticula. The collagen fibers were smaller in number and did not form collagen bundles as thick as those shown in the treatment groups.

#### 3.4.4. Immunohistochemistry results

In the immunohistochemical staining results, no significant changes in MMP-1 or MMP-2 were observed between the baseline and 2 weeks post-treatment specimens in all groups. However, there were noticeable increases in TIMP-1 and TIMP-2 in degrees which varied according to the different groups. The most marked increase of TIMP-1 was observed in group 3 (Fig. 8a), while that of TIMP-2 was shown in group 2 (Fig. 8b). We could find a slight increase of TIMP-1 and 2 in the control group as well, the degree of which was much less than those in the treatment groups.

#### 3.4.5. Biochemical changes (real time RT-PCR results, Table 5)

The comparison of the mRNA levels of IL-1 $\beta$  between before treatment and 20 minutes after the final treatment demonstrated a marked increase in group 1 and group 3 in the post-treatment specimens, the levels of which were 13.3 and 13.7 times higher than those of before treatment,

respectively. In group 2, the post-treatment IL-1 $\beta$  mRNA level was 6.2 times higher compared with before treatment. On the other hand, in the control group, the post-treatment level of IL-1 $\beta$  mRNA was only 1.59 times higher than before treatment.

In regards to TNF- $\alpha$ , the results also showed an increase in its mRNA levels in the post-treatment specimens, although more moderately than that of IL-1 $\beta$ . The mRNA levels were 1.6-, 1.36-, and 2.5-fold those of the baseline after treatment with 830 nm alone, 633 nm alone, and a combination of 830 and 633 nm, respectively. Similar to IL-1 $\beta$ , TNF- $\alpha$  mRNA levels showed a greater increase when infrared light was used, compared to when red light was used alone, even though the difference was not as marked as that observed in the case of IL-1 $\beta$ . In the control group, the post-treatment mRNA level of TNF- $\alpha$  decreased to 0.38-fold that of the baseline level.

The mRNA levels of IL-6 decreased after treatment. They were 0.14, 0.5 and 0.74-fold of those of baseline after treatment with 830 nm alone, 633 nm alone, and a combination of 830 and 633 nm, respectively. No patterns relating to the wavelength of light was observed. In the control group, the levels of IL-6 mRNA in the post-treatment specimens also decreased 0.26-fold, which made the interpretation of these data difficult.

The mRNA levels of ICAM-1 increased slightly after treatment with 830 nm alone (1.39-fold), whereas they

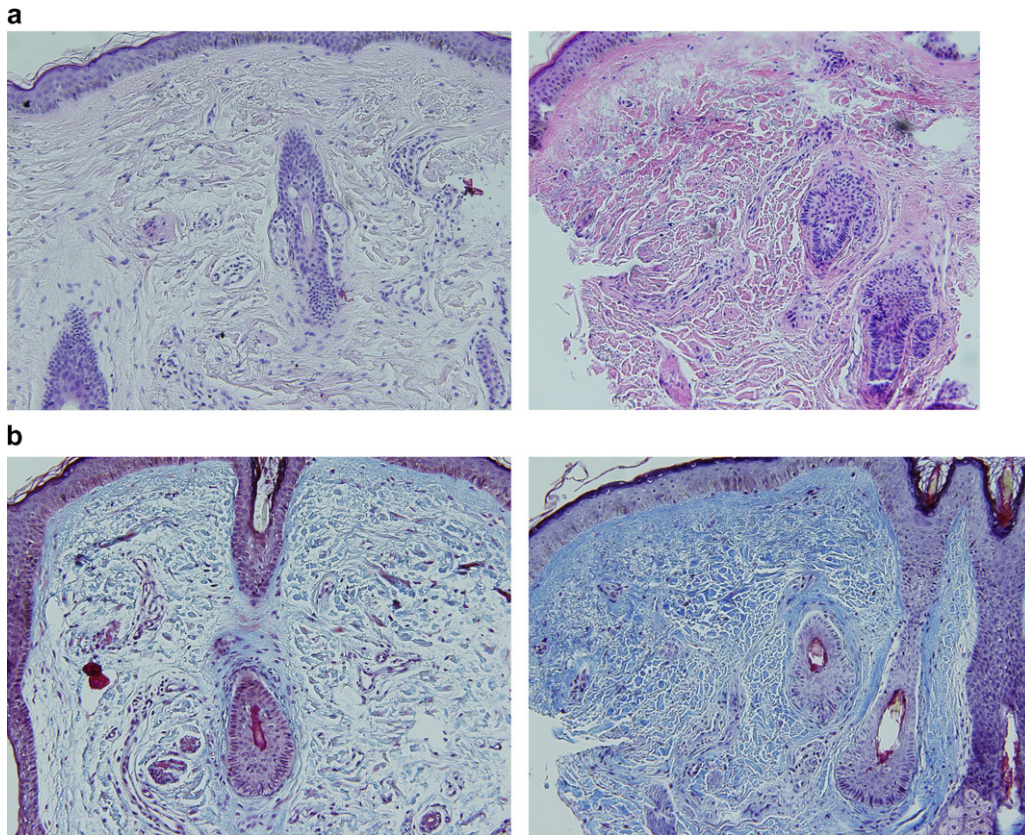


Fig. 5. In the treatment groups, a significant increase in the amount of collagen was observed by histologic evaluation with standard preparation with H & E (a). This finding was confirmed by Masson-trichrome stain for collagen (b) (x 200 for all). (a) Left: Before treatment, Right: 2 weeks after treatment completion (b) Left: Before treatment, Right: 2 weeks after treatment completion.

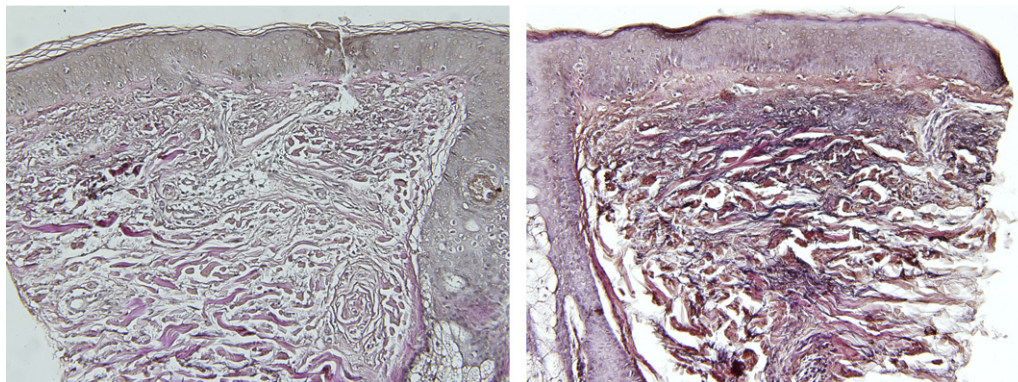


Fig. 6. A significant increase in the amount of elastic fibers was observed in the treatment groups (Verhoeff-van Gieson stain, x 200). Left: Before treatment, Right: 2 weeks after treatment completion.

decreased mildly after 633 nm alone treatment (0.54-fold). After the combination therapy with 830 and 633 nm, however, the levels were 5.39-fold those of the baseline. The pattern of the levels being higher with the use of infrared light was similar to that of TNF- $\alpha$ . The level of ICAM-1 mRNA decreased after sham treatment, 0.4-fold that of the baseline.

The changes in the mRNA levels of Cx43 revealed an increase after treatment. They were 1.31, 2.53, and 2.42-fold times those of the baseline after treatment with 830 nm alone, 633 nm alone, and a combination of 830

and 633 nm, respectively. Unlike IL-1 $\beta$ , TNF- $\alpha$ , or ICAM-1, the degree of increase was highest when 633 nm was used alone. The Cx 43 mRNA level was 0.92-fold that of baseline after the sham treatment.

#### 4. Discussion

Most nonablative rejuvenation technologies are designed to produce controlled amounts of thermal damage to the dermis, that is, a subclinical wounding, to invoke the wound healing process which leads to biosynthesis of new collagen

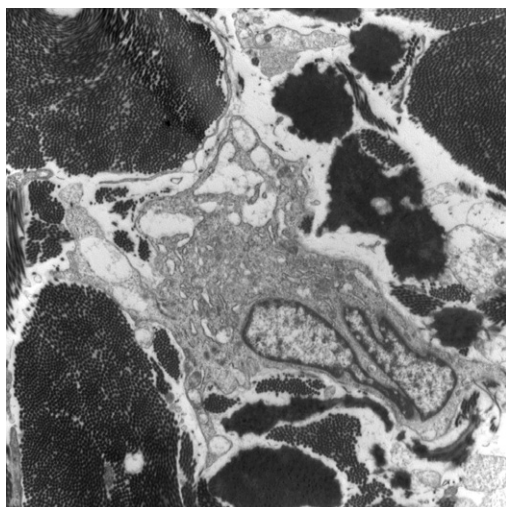


Fig. 7. Transmission electromicroscopic findings showed activated fibroblasts with numerous dilated endoplasmic reticula surrounded by abundant collagen fibers in the treatment groups (x 8,000).

[10–24,38]. A proper amount and penetration depth of the controlled photothermal damage is considered to be vital for effective induction of collagen synthesis [23, 24,39].

The use of LEDs for skin rejuvenation is unique in that it does not produce any thermal damage. Instead of photothermal damaging, it induces a photobiomodulative reaction [25–29]. Photobiomodulation is considered to stimulate fibroblast proliferation, collagen synthesis, growth factors and extracellular matrix production and enhances cutaneous microcirculation through activating the mitochondrial respiratory system of the cells [25–36]. The beneficial effects of a new generation of powerful and quasimonochromatic LEDs were first reported by Whelan et al. [30–32], who have demonstrated that 670 nm LED treatment up-regulated tissue regeneration genes and accelerated wound closure by stimulating cell activities. Rapid development of both LED-based devices and their application has now enabled LED therapy to be used for skin rejuvenation by utilizing its effectiveness in inducing photobiomodulation. Some clinical studies have shown the efficacy of 590 nm pulsed LEDs in improving photoaged skin through increasing collagen precursors [27]. The clinical efficacy of 633 nm and 830 nm LEDs for skin rejuvenation has also been reported in some articles [28,29].

However, well-designed clinical studies have been very sparse, which have used split-face exposures performed in a randomized, double-blinded, placebo-controlled trial with repeated and quantitative measures of response [12]. The mechanism of action of LED phototherapy in skin rejuvenation has also not yet been investigated vigorously. In the present study, we tried to determine the clinical efficacy of LED phototherapy for skin rejuvenation through an objective methodology utilizing a controlled, double-blinded and hemi-face model. We also investigated the histological and ultrastructural changes and alterations in the primary cytokines and enzymes that are known to be

affected by other nonablative rejuvenation procedures. The use of profilometry and other instrumental measurements enabled us to obtain objective data of the clinical efficacy, which were not observer-dependent and made it possible to compare the therapeutic effects between different treatment parameters.

The results revealed a statistically significant improvement in the representative values of wrinkle severity and skin elasticity between baseline and 3 months after treatment completion in the treatment groups, with skin elasticity first tending to show an apparent improvement in treatment week 3. Both sets of values exhibited continued improvement, even during progressive treatment-free follow up assessments. This improvement was not observed in the control group, with a statistically significant difference in the percentage improvements between the control group and the treatment groups. In addition, the within-patient comparison between the treated and the covered sides in the same individual revealed a statistically significant improvement in wrinkles and skin elasticity only in the treated side, whereas no such changes were noted in the covered side. This ‘double comparison’ methodology allowed us to confirm the improvements in severity of wrinkles and skin elasticity after LED phototherapy in a more objective fashion.

Another important reason we set an additional control group in a split-face study was to avoid the bias which might be caused by the possible influence of a paracrine, or a bystander effect. It has been suggested that, in light therapy, photons may stimulate cells to release cytokines [17,30–36,40]. We took the possibility into account that paracrine or bystander signaling agents, such as cytokines or growth factors, might diffuse into the dermis or circulate through the dermal vasculature from the treated side to the non-treated side. In such case of negation of the hemiface model, where any existing difference between the treated and covered sides would become indistinguishable, comparison between the treatment groups and the sham irradiated control group would give another tool for assessment of the therapeutic efficacy.

The subjects in the three treatment groups expressed satisfaction with LED phototherapy as the follow-up period progressed. They reported overall improvements in the skin tone, texture, firmness and tightness as well as the severity of wrinkles. On the contrary, most of the patients in the control group could not find any perceptible advantages, even by the final assessment session. The dissatisfaction of patients in the control group resulted in the highest drop-out rate among all of the study groups. The investigators’ assessments showed a good correlation with the subjects’ assessments (Table 4).

The specimens for histological and ultrastructural evaluations were obtained two weeks post-treatment, because the changes in the dermal matrix is known to become prominent 10–20 days after a rejuvenation procedure [20,41]. On the other hand, biochemical responses such as cytokine release are known to be acutely induced by the rejuvenation therapy and last for several hours to a few days [7,20,42,43].

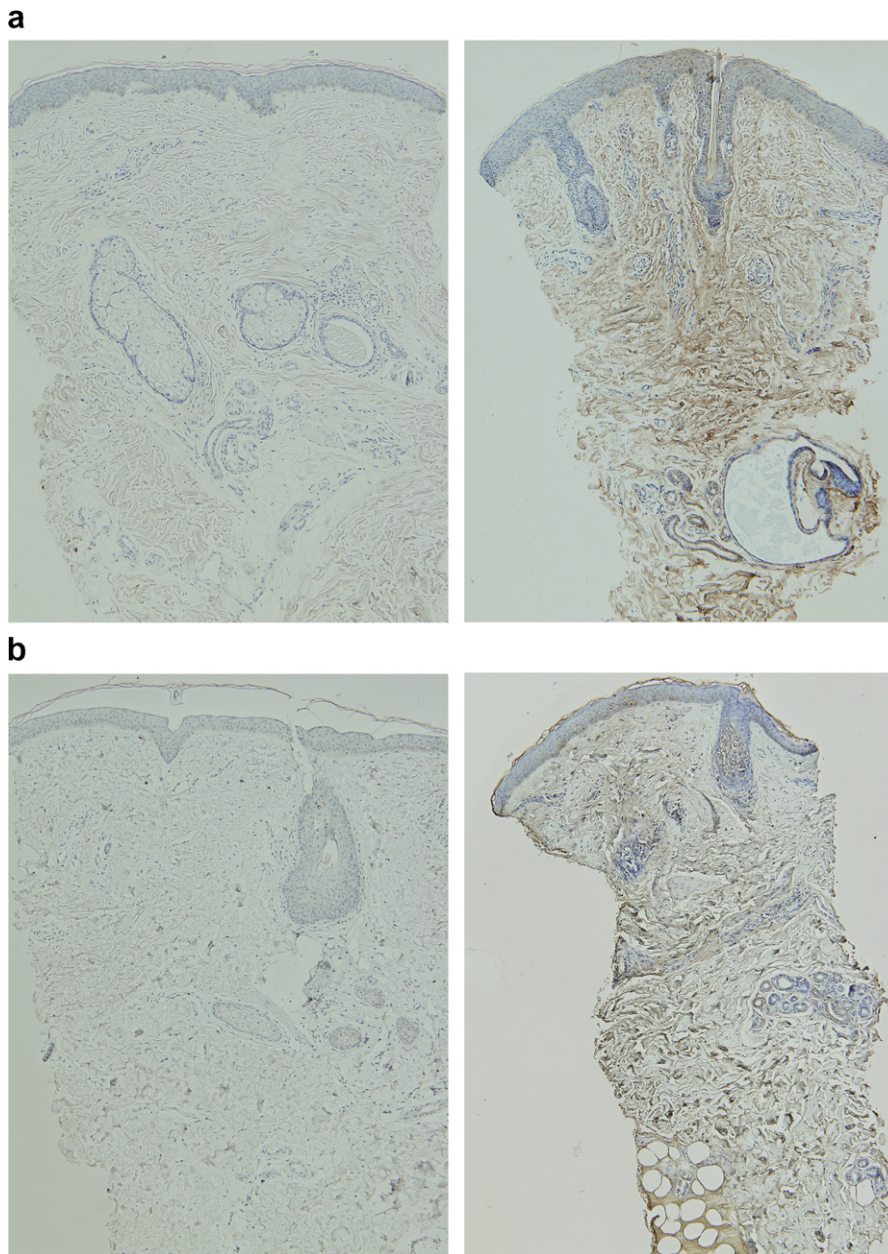


Fig. 8. Immunohistochemical staining showed noticeable increases in TIMP-1 (a) and TIMP-2 (b) at various degrees in the treatment groups (x 100 for all. The pictures of post-treatment specimens appear smaller than those of pre-treatment specimens, because the post-treatment specimens were split into two pieces to be processed in parallel for TEM).

Therefore, specimens for biochemical evaluation were obtained 20 minutes after the final treatment.

On histological examination of these specimens, the increase in the amount of collagen was well-evidently demonstrated in the post-treatment specimens, which was correspondent with the results of other studies using 590 nm LED or other non-ablative rejuvenation modalities [13–16,19,21,23,24,27]. The noticeable difference between our results and those of other studies was the depth and range of the increase of collagen. It is known that induction of collagen synthesis by nonablative rejuvenation procedures occurs largely in the papillary and upper reticular dermis, forming the so-called Grenz zone [39,44]. The depth of this

actively responding area is considered to be around 100–500  $\mu\text{m}$  below the DEJ [39,44]. Therefore, most photothermally-based nonablative rejuvenation technologies aim to deliver thermal damage to that depth within the dermis to get the maximal effects [23,24,39,44]. As in other studies, the formation of the Grenz zone was found also in our study. However, in our results, the depth of changes in collagen, presented as increases in the amount and thickening of collagen bundles, and packing of the arrangement of the collagen network, appeared deeper than 500  $\mu\text{m}$  extending to almost the entire dermis, not being limited to the papillary and upper reticular dermis as shown in other studies. In addition, not corresponding with the current consensus

Table 5

Real time RT-PCR results showed a noticeable increase in the mRNA levels of IL-1 $\beta$ , TNF- $\alpha$ , and Connexin 43 in the treatment groups. The changes in the mRNA levels of IL-6 and ICAM-1 did not show a consistent tendency

	Group 1 (830 nm alone)	Group 2 (633 nm alone)	Group 3 (830 nm and 633 nm)	Group 4 (Control sham light)
IL-1 $\beta$	13.3	6.165	13.7	1.59
TNF- $\alpha$	1.6	1.36	2.5	0.38
IL-6	0.14	0.5	0.74	0.26
ICAM-1	1.39	0.54	5.39	0.43
Connexin-43	1.31	2.53	2.42	0.92

Values are fold change from baseline.

that the dermal matrix remodeling is limited to the areas which are directly or indirectly affected by thermal damage by the nonablative rejuvenation devices [38,39], our study results revealed dermal changes even in an area deeper than the usually agreed optical penetration depth of 633 nm (550  $\mu$ m) [45], although 830 nm is associated with much deeper penetration than 633 nm. It is unique that these changes were actually obtained without causing any thermal damage to the dermis, using a non-thermal LED light source, which we consider is a significant point of our results. The post-treatment TEM findings revealed highly activated fibroblasts containing increased numbers of dilated endoplasmic reticula and surrounded by abundant thickened collagen bundles and elastic fibers, which may probably be the source of the dermal matrix changes producing increased amounts of collagen and elastic fibers.

In the present study, increases were noted in elastic fibers in addition to collagen fibers, after LED phototherapy. This finding also corresponds with other nonablative rejuvenation studies [19,20]. Although increased numbers of elastic fibers have also been found in photodamaged skin, such fibres demonstrate degenerative elastotic changes. However, in our study, Alcian blue staining ruled out this possibility, showing no evidence of deposition of acid mucopolysaccharides, which are known to exist in a large amount in elastotic material [46]. In addition, the elastic fibers shown in the TEM findings appeared normal-structured, containing amorphous, electrolucent elastin in the center with numerous fine microfibrils embedded largely in the periphery of the elastin, arranged parallel to the long-axis of the elastic fiber [47]. It is possible that this significant increase in elastic fibers may play a role in rejuvenating photoaged skin through improving the skin elasticity and resilience, as seen in the objective Cutometer<sup>TM</sup> data, although this hypothesis is yet to be confirmed by further studies.

The significant decrease of melanin levels after red LED irradiation has been already observed in our previous clinical study on acne treatment [48]. In addition, many subjects spontaneously reported their perception of brightening of the skin tone in the present study, as had been also the case in the previous study. We performed Schmorl's staining to elucidate any changes in the amount of melanin pigment between before and after treatment,

but could not find any significant difference. We hypothesize that the decrease in the melanin levels measured by Mexameter<sup>TM</sup> were possibly as the result of reasons other than the direct decrease in the amount of melanin pigment, for example, changes in the reflection of light from the epidermis or alteration in the absorption and scattering characteristics of light in the dermis. Because the Mexameter<sup>TM</sup> quantifies melanin pigmentation by comparing the amount of reflected light to that of a device-generated reference beam [49], morphological changes in the epidermis and even in the dermis may alter this reflected beam and cause a decrease in the measured levels without any actual decrease in the total melanin amount. Further studies with larger sample sizes and various biologic investigations will be necessary to find out the mechanism of action of improvement of the skin tone by red LED phototherapy.

Of particular interest in our study was that the pro-inflammatory cytokines, IL-1 $\beta$  and TNF- $\alpha$ , were induced by non-thermal LED treatment. It has been suggested that these primary cytokines are produced by inflammatory cells which are recruited to heal the intentionally formed photothermally-mediated wounds associated with laser treatments, and that this cascade of wound healing consequently contributes to new collagen synthesis [7,20,22,42,50]. Our results suggest that LED therapy may be useful to induce this wound healing process, through the athermal and atraumatic induction of a subclinical 'quasi-wound', even without any actual wounding by thermal damage which can cause complications as shown in other thermal laser treatments.

Some investigations have demonstrated that proteolytic clearance of photodamaged, fragmented collagen by MMPs might facilitate biosynthesis of new collagen [42]. Although we did not measure the amount of MMP-1 and MMP-2 early after LED therapy, we observed that there were not any significant changes in their status in the 2 weeks post-treatment specimens. It is not clear whether MMPs were not induced at all by LED therapy or if they were induced earlier after the therapy and decreased again to baseline during the subsequent 2 weeks. However, it is highly probable that MMPs might be induced in the early response, because IL-1 $\beta$  and TNF- $\alpha$ , which were shown to be increased by LED therapy in our results, are cytokines that induce production of MMPs.

Additionally, our results revealed a significant increase in the amount of TIMP-1 and TIMP-2 two weeks after LED therapy, which led us to hypothesize that the remarkable increase in the amount of collagen shown in the histologic evaluation might be related to induction of TIMPs because of their action of inhibiting MMP activities.

Putting together these observations, we hypothesize that increased production of IL-1 $\beta$  and TNF- $\alpha$  might have induced MMPs in the early response to LED therapy, which might clear the photodamaged collagen fragments to facilitate biosynthesis of new collagen fibers, and that subsequent events of normalization of MMPs status and increase in the amount of TIMPs might protect the newly

synthesized collagen from proteolytic degradation by MMPs. Future studies involving serial quantification of MMPs and TIMPs are merited to understand their roles in dermal matrix remodeling after LED therapy.

There are some limitations in interpreting the changes in IL-6 and ICAM-1 because of the lack of consistency. IL-6 is known to increase in the acute inflammatory phase and to be induced by IL-1 $\beta$  and TNF- $\alpha$  [51,52]. This does not correspond with our results, as the level of IL-6 decreased despite the increase of IL-1 $\beta$  and TNF- $\alpha$ . On the other hand, ICAM-1 is known to mediate the antigen recognition process of T cells and leukocyte-endothelial cell interaction, and to elevate the inflammatory response through helping the extravasation of immune cells to recruit them to the target sites [53–56]. This adhesion molecule is also induced by IL-1 $\beta$  and TNF- $\alpha$  [56]. Our results showed increases of ICAM-1 in group 1 and 3, but a decrease in group 2, in spite of the increase of the primary cytokines. More data from a study using a larger sample size are needed to investigate changes in IL-6 and ICAM-1 after LED phototherapy.

Gap junctional intercellular communication (GJIC) by connexin channels is known to be vital for maintaining tissue homeostasis, growth control, development and synchronized response of cells to stimuli [57–60]. Cx43 is the main protein of which gap junctions are composed [57,59]. In human skin, Cx43 is primarily located in the interfollicular epidermis, throughout the spinous and granular cell layers and focally in the basal cell layer, and is also expressed in dermal fibroblasts, hair follicles, smooth muscle cells and endothelial cells [57]. Various kinds of skin tumors, including melanoma, are known to express decreased levels of Cx43 than normal skin [57,61–63]. During the early wound healing process, up-regulation of Cx43 is observed in smooth muscle cells and endothelial cells in the dermis, which is considered to mediate transendothelial migration of leukocytes through GJIC [57,64,65]. An *in vitro* study using normal human dermal fibroblast suggested that the increase of Cx43 expression may enhance GJIC, which results in improvement of the tissue strength [66].

In our study, the elevation of Cx43 mRNA was found in all treatment groups. Because light at 633 nm and 830 nm penetrates the epidermis and largely affects the dermis, it can be postulated that the increased Cx43 might be expressed by dermal components such as fibroblasts, hair follicle cells, or endothelial cells. It is our assumption that the increased expression of Cx43 might enhance cell-cell communication between these dermal components, especially the fibroblasts, and make them synchronize the cellular responses to the photobiostimulation effects from LED treatment to produce new collagen throughout a more extensive area, even in those areas not irradiated directly. We consider that this hypothesis may explain one of the reasons for the extensive increase of collagen in the entire dermis shown in our histological findings, where the dermal matrix remodeling appeared to have occurred in sites other than the directly stimulated region.

Our hypothesis mentioned above can be understood in a similar context with the bystander effect theory. The bystander effect refers to a phenomenon where biological changes as a result of ionizing radiation occur also in cells that are not directly irradiated by the incident radiation [67]. So far this phenomenon has been mainly investigated in radiotherapy for cancers. In addition, there was an *in vivo* study which demonstrated that low-energy laser radiation-mediated enhanced wound healing had been observed in regions other than the directly irradiated sites, suggesting that the bystander effect may also occur in beneficial biological events [40]. The current understanding of the bystander effect is that irradiated cells may secrete intercellular signaling molecules or that the gap junctional communication between irradiated cells and non-irradiated cells may play an important role in causing this phenomenon [67]. In the present study, we have demonstrated an induction of biologic signaling molecules such as pro-inflammatory cytokines and that of a major gap junction protein, which may suggest an enhanced gap junctional communication, after LED phototherapy. Therefore, it can be postulated that these changes might be a reflection of the LED therapy-mediated bystander effect, which might propagate the photobiomodulation effect between cells, even into the deeper dermis, and bring about the histological alterations of collagen and elastic fiber production to the dramatically large extent as illustrated by the histology in the present study. Further studies are necessary to verify our hypothesis and to investigate the exact mechanisms of action of LED photobiomodulation effects.

Comparison of clinical efficacy between the three different treatment protocols showed some characteristics in each measured property. In terms of wrinkle severity, the percentage reduction was greatest after a combination of 830 and 633 nm LED treatment (group 3), while skin elasticity increased most remarkably after 830 nm alone treatment (group 1). On the other hand, the reduction of the amount of melanin was observed only after treatment with 633 nm alone (group 2), and the patients' satisfaction about skin brightening was also reported largely in group 2 (data not shown). In terms of the subjective global assessment, the proportion of highly satisfied patients with this therapy was highest in groups 1 and 3 in both of which the infrared LED head was used. Considering that skin rejuvenation aims at both wrinkle reduction and improvement of skin tone, we consider that the combination of 830 and 633 nm LED treatment would offer the best clinical effectiveness by combining the different bioadvantages produced by these two wavelengths of light. Further studies will be merited to optimize the treatment protocols for LED phototherapy for skin rejuvenation.

## 5. Conclusions

Our study results showed that LED phototherapy is an effective treatment for skin rejuvenation through objectively measured data and histological and ultrastructural

bodies of evidence of increased collagen and elastic fibers as well as clinical photographs and double-blinded assessment of the investigators and the subjects. A notable increase of TIMP-1 and 2 was observed in the immunohistochemical staining, which suggested that altered enzymatic activity related to the dermal matrix remodeling may play a role in the mechanism of action of LED phototherapy. Particularly, it is notable that LED phototherapy, which does not cause any thermal or chemical damaging, induced proinflammatory cytokines just as in photothermally-mediated nonablative skin rejuvenation, which we consider consequently led to the biosynthesis of new collagen within the dermis. More importantly, these histological changes occurred deeper than 100–500  $\mu\text{m}$  below the DEJ, the actively responding area to most nonablative laser treatments, and hence their target zone, and in addition deeper than the classically-accepted optical penetration depth of at least the visible red wavelength. We hypothesize that this result might be caused by an extensive cellular response to the photobiomodulative effect of LED therapy through enhanced gap junctional intercellular communication, even though the sample size was too small to draw a clear conclusion. Further studies with larger sample sizes and repeated follow-up biopsies are merited to investigate the exact changes and roles of these biologic effectors in the dermal remodeling process after LED phototherapy.

We concluded that 830 nm and 633 nm LED phototherapy is an effective, safe, well-tolerated and painless treatment for skin rejuvenation. From the clinical aspect, the non-thermal feature of LED phototherapy may be a significant advantage, because we could achieve effective rejuvenation of aging skin without inducing any thermal damage or wound in normal skin. We recommend the use of the combination of these two wavelengths of light to maximize the effect through utilizing the advantages specific to each wavelength.

## 6. Abbreviations

CO <sub>2</sub>	carbon dioxide
Cx43	connexin-43
DEJ	dermoepidermal junction
Er:YAG	erbium: yttrium-aluminum-garnet
GJIC	gap junctional intercellular communication
H & E	hematoxylin and eosin
ICAM-1	intercellular adhesion molecule-1
IL-1 $\beta$	interleukin-1 $\beta$
IL-6	interleukin-6
IPL	intense pulsed light
KTP	potassium-titanyl-phosphate
LED	light-emitting diode
MMP	matrix metalloproteinase
mRNA	messenger ribonucleic acid
Nd:YAG	neodymium: yttrium-aluminum-garnet
PBS	phosphate buffered saline
PDL	pulsed dye lasers
RM-ANOVA	repeated measures of analysis of variance

RT-PCR	reverse transcriptase-polymerase chain reaction
TBS	tris-buffered saline
TEM	transmission electromicroscopy
TIMP	tissue inhibitor of matrix metalloproteinase
TNF- $\alpha$	tumor necrosis factor- $\alpha$

## 7. Disclosure of conflicts of interest

Photo Therapeutics Ltd. supported the costs of only the electromicroscopic examination, immunohistochemical staining and real time RT-PCR processes. The authors have not received any funds toward the plan or conduction of this study. We certify that we have no affiliation with or financial involvement in any organization or entity with a direct or indirect financial interest in the subject matter or materials discussed in the manuscript.

## Acknowledgement

We wish to thank Photo Therapeutics Ltd., Fazely, Tamworth, UK, for generously making available the LED-based Omnilux<sup>TM</sup> devices used in this study at no cost. We are also deeply grateful to Antonius R. Soelistyo, B. Tech (hons), for his kindness to help us with performing this study and to R. Glen Calderhead, MSc, PhD(MedSci), FRSM, for the English proofreading of this paper.

## References

- [1] J.L. Bologna, Aging skin, *Am. J. Med.* 98 (suppl 1A) (1995) S99–S103.
- [2] C.E.M. Griffiths, The clinical identification and quantification of photodamage, *Br. J. Dermatol.* 127 (suppl 41) (1992) S37–S42.
- [3] L.H. Kligman, Photoaging. Manifestations, prevention, and treatment, *Clin. Geriatr. Med.* 5 (1989) 235–251.
- [4] Y. Takema, Y. Yorimoto, M. Kawai, G. Imokawa, Age related changes in the elastic properties and thickness of human facial skin, *Br. J. Dermatol.* 131 (1994) 641–648.
- [5] G.H. Branham, J.R. Thomas, Rejuvenation of the skin surface: chemical peel and dermabrasion, *Facial. Plast. Surg.* 12 (1996) 125–133.
- [6] L.E. Airan, G.J. Hruza, Current lasers in skin resurfacing, *Facial. Plast. Surg. Clin. North. Am.* 13 (2005) 127–139.
- [7] J.S. Orringer, S. Kang, T.M. Johnson, D.J. Karimipour, T. Hamilton, C. Hammerberg, J.J. Voorhees, G.J. Fisher, Connective tissue remodeling induced by carbon dioxide laser resurfacing of photo-damaged human skin, *Arch. Dermatol.* 140 (2004) 1326–1332.
- [8] C.A. Nanni, T.S. Alster, Complications of carbon dioxide laser resurfacing: an evaluation of 500 patients, *Dermatol. Surg.* 24 (1998) 315–320.
- [9] S. Sriprachya-Anunt, R.E. Fitzpatrick, M.P. Goldman, S.R. Smith, Infections complicating pulsed carbon dioxide laser resurfacing for photoaged skin, *Dermatol. Surg.* 23 (1997) 527–535.
- [10] C.A. Hardaway, E.V. Ross, Nonablative laser skin remodeling, *Dermatol. Clin.* 20 (2002) 97–111.
- [11] R.A. Weiss, D.H. McDaniel, R.G. Geronemus, Review of nonablative photorejuvenation: reversal of the aging effects of the sun and environmental damage using laser and light sources, *Semin. Cutan. Med. Surg.* 22 (2003) 93–106.
- [12] C.C. Dierickx, R.R. Anderson, Visible light treatment of photoaging, *Dermatol. Ther.* 18 (2005) 191–208.

- [13] D.J. Goldberg, New collagen formation after dermal remodeling with an intense pulsed light source, *J. Cutan. Laser. Ther.* 2 (2000) 59–61.
- [14] E. Hernandez-Perez, E.V. Ibiert, Gross and microscopic findings in patients submitted to nonablative full-face resurfacing using intense pulsed light: a preliminary study, *Dermatol. Surg.* 28 (2002) 651–655.
- [15] M.A. Trelles, I. Allones, M. Velez, Non-ablative facial skin photo-rejuvenation with an intense pulsed light system and adjunctive epidermal care, *Lasers. Med. Sci.* 18 (2003) 104–111.
- [16] B.D. Zelickson, S.L. Kilmer, E. Bernstein, V.A. Chotzen, J. Dock, D. Mehregan, C. Coles, Pulsed dye laser therapy for sun damaged skin, *Lasers. Surg. Med.* 25 (1999) 229–236.
- [17] P. Bjerring, M. Clement, L. Heickendorff, H. Egevist, M. Kiernan, Selective non-ablative wrinkle reduction by laser, *J. Cutan. Laser. Ther.* 2 (2000) 9–15.
- [18] P. Bjerring, M. Clement, L. Heickendorff, H. Lybecker, M. Kiernan, Dermal collagen production following irradiation by dye laser and broad band light source, *J. Cosmet. Laser. Ther.* 3 (2001) 39–43.
- [19] E. Rostan, L.E. Bowes, S. Iyer, R.E. Fitzpatrick, A double-blind side-by-side comparison study of low fluence long pulse dye laser to coolant treatment for wrinkling of the cheeks, *J. Cosmet. Laser. Ther.* 3 (2001) 129–136.
- [20] T. Omi, S. Kawana, S. Sato, M. Honda, Ultrastructural changes elicited by a non-ablative wrinkle reduction laser, *Lasers. Surg. Med.* 32 (2003) 46–49.
- [21] D.J. Goldberg, D. Sarradet, M. Hussain, A. Krishtul, R. Phelps, Clinical, histologic and ultrastructural changes after nonablative treatment with a 595-nm flashlamp-pumped pulsed dye laser: comparison of varying settings, *Dermatol. Surg.* 30 (2004) 979–982.
- [22] A. Fatemi, M.A. Weiss, R.A. Weiss, Short-term histologic effects of nonablative resurfacing: results with a dynamically cooled millisecond-domain 1320 nm Nd:YAG laser, *Dermatol. Surg.* 28 (2002) 172–176.
- [23] M.A. Trelles, I. Allones, J.L. Levy, R.G. Calderhead, G.A. Moreno-Arias, Combined nonablative skin rejuvenation with the 595- and 1450-nm lasers, *Dermatol. Surg.* 30 (2004) 1292–1298.
- [24] E.V. Ross, F.P. Sajben, J. Hsia, D. Barnette, C.H. Miller, J.R. McKinlay, Nonablative skin remodeling: selective dermal heating with a mid-infrared laser and contact cooling combination, *Lasers. Surg. Med.* 26 (2000) 186–195.
- [25] R.A. Weiss, M.A. Weiss, R.G. Geronemus, D.H. McDaniel, A novel non-thermal non-ablative full panel LED photomodulation device for reversal of photoaging: digital microscopic and clinical results in various skin types, *J. Drugs. Dermatol.* 3 (2004) 605–610.
- [26] R.A. Weiss, D.H. McDaniel, R.G. Geronemus, M.A. Weiss, K.L. Beasley, G.M. Munavalli, S.G. Bellew, Clinical experience with light-emitting diode (LED) photomodulation, *Dermatol. Surg.* 31 (2005) 1199–1205.
- [27] R.A. Weiss, D.H. McDaniel, R.G. Geronemus, M.A. Weiss, Clinical trial of a novel non-thermal LED array for reversal of photoaging: clinical, histologic, and surface profilometric results, *Lasers. Surg. Med.* 36 (2005) 85–91.
- [28] J. Bhat, J. Birch, C. Whitehurst, S.W. Lanigan, A single-blinded randomised controlled study to determine the efficacy of Omnilux revive facial treatment in skin rejuvenation, *Lasers. Med. Sci.* 20 (2005) 6–10.
- [29] B.A. Russell, N. Kellett, L.R. Reilly, A study to determine the efficacy of combination LED light therapy (633 nm and 830 nm) in facial skin rejuvenation, *J. Cosmet. Laser. Ther.* 7 (2005) 196–200.
- [30] H.T. Whelan, R.L. Smits Jr., E.V. Buchman, N.T. Whelan, S.G. Turner, D.A. Margolis, V. Cevenini, H. Stinson, R. Ignatius, T. Martin, J. Cwiklinski, A.F. Philippi, W.R. Graf, B. Hodgson, L. Gould, M. Kane, G. Chen, J. Caviness, Effect of NASA light-emitting diode irradiation on wound healing, *J. Clin. Laser. Med. Surg.* 19 (2001) 305–314.
- [31] H.T. Whelan, J.F. Connelly, B.D. Hodgson, L. Barbeau, A.C. Post, G. Bullard, E.V. Buchmann, M. Kane, N.T. Whelan, A. Warwick, D. Margolis, NASA light-emitting diodes for the prevention of oral mucositis in pediatric bone marrow transplant patients, *J. Clin. Laser. Med. Surg.* 20 (2002) 319–324.
- [32] H.T. Whelan, E.V. Buchman, A. Dhokalia, M.P. Kane, N.T. Whelan, M.T. Wong-Riley, J.T. Eells, L.J. Gould, R. Hammamieh, R. Das, M. Jett, Effect of NASA light-emitting diode irradiation on molecular changes for wound healing in diabetic mice, *J. Clin. Laser. Med. Surg.* 21 (2003) 67–74.
- [33] T.I. Karu, Photobiological fundamentals of low-power laser therapy, *J. Quantum. Electron.* 23 (1987) 1703–1717.
- [34] T. Karu, Primary and secondary mechanisms of action of visible to near-IR radiation on cells, *J. Photochem. Photobiol. B, Biol.* 49 (1999) 1–17.
- [35] T.S. Lam, R.P. Abergel, C.A. Meeker, J.C. Castel, R.M. Dwyer, J. Uitto, Laser stimulation of collagen synthesis in human skin fibroblast cultures, *Laser. Life. Sci.* 1 (1986) 61–77.
- [36] S. Young, P. Bolton, M. Dyson, W. Harvey, C. Diamantopoulos, Macrophage responsiveness to light therapy, *Lasers. Surg. Med.* 9 (1989) 497–505.
- [37] J. Cohen, Statistical power analysis for behavioral sciences, second ed., Lawrence & Earlbaum, New Jersey, 1998.
- [38] E.V. Ross, B.D. Zelickson, Biophysics of nonablative dermal remodeling, *Semin. Cutan. Med. Surg.* 21 (2002) 251–265.
- [39] J.S. Nelson, B. Majaron, K.M. Kelly, What is nonablative photorejuvenation of human skin? *Semin. Cutan. Med. Surg.* 21 (2002) 238–250.
- [40] E. Mester, A.F. Mester, A. Mester, The biomedical effects of laser application, *Lasers. Surg. Med.* 5 (1985) 31–39.
- [41] R. Ross, E.P. Benditt, Wound healing and collagen formation. I. Sequential changes in components of guinea pig skin wounds observed in the electron microscope, *J. Biophys. Biochem. Cytol.* 11 (1961) 677–700.
- [42] J.S. Orringer, J.J. Voorhees, T. Hamilton, C. Hammerberg, S. Kang, T.M. Johnson, D.J. Karimipour, G. Fisher, Dermal matrix remodeling after nonablative laser therapy, *J. Am. Acad. Dermatol.* 53 (2005) 775–782.
- [43] J.M. McPherson, K.A. Pietz, Collagen in dermal wound repair, In: *Biology of wound repair*, Plenum, New York, pp. 471–496.
- [44] C.A. Hardaway, E.V. Ross, D.J. Barnette, D.Y. Paithankar, Non-ablative cutaneous remodeling with a 1.45 microm mid-infrared diode laser: phase I, *J. Cosmet. Laser. Ther.* 4 (2002) 3–8.
- [45] E.V. Ross, Optical treatments for acne, *Dermatol. Ther.* 18 (2005) 253–266.
- [46] W.M. Sams Jr., J.G. Smith Jr., The histochemistry of chronically sun-damaged skin. An investigation of mucopolysaccharides and basophilic in actinically damaged skin using alcian blue, mowry's, and Hicks-Matthaei stains, methylation, and saponification, *J. Invest. Dermatol.* 37 (1961) 447–453.
- [47] F.N. Ghadially, Elastic fibres, elaunin fibres and oxytalan fibres, in: *Ultrastructural pathology of the cell and matrix- A textbook and atlas of physiological and pathological alterations in the fine structure of cellular and extracellular components*, Butterworths, London, 1988, pp. 1252–1259.
- [48] S.Y. Lee, C.E. You, M.Y. Park, Blue and red light combination LED phototherapy for acne vulgaris in patients with skin phototype IV, *Lasers. Surg. Med.* 39 (2007) 180–188.
- [49] P. Clarys, K. Alewaeters, R. Lambrecht, A.O. Barel, Skin color measurements: comparison between three instruments: the Chromameter®, the DermaSpectrometer® and the Mexameter®, *Skin. Res. Technol.* 6 (2000) 230–238.
- [50] C.C. Chua, B.H.L. Chua, Tumor necrosis factor- $\alpha$  induces mRNA for collagenase and TIMP in human skin fibroblasts, *Connect. Tissue. Res.* 25 (1990) 161–170.
- [51] X.P. Wang, M. Schunck, K.J. Kallen, C. Neuman, C. Trautwein, S. Rose-John, E. Proksch, The interleukin-6 cytokine system regulates epidermal permeability barrier homeostasis, *J. Invest. Dermatol.* 123 (2004) 124–131.
- [52] K. Turksen, T. Kupper, L. Degenstein, I. Williams, E. Fuchs, Interleukin 6: insights to its function in skin by overexpression in transgenic mice, *Proc. Natl. Acad. Sci. USA.* 89 (1992) 5068–5072.

- [53] S.M. Albelda, Endothelial and epithelial cell adhesion molecules, *Am. J. Respir. Cell. Mol. Biol.* 4 (1991) 195–203.
- [54] T. Nagaoka, Y. Kaburagi, Y. Hamaguchi, M. Hasegawa, K. Takehara, D.A. Steeber, T.F. Tedder, S. Sato, Delayed wound healing in the absence of intercellular adhesion molecule-1 or L-selectin expression, *Am. J. Pathol.* 157 (2000) 237–247.
- [55] A.K. Abbas, A.H. Lichtman, J.S. Pober, Cytokines, in: *Cellular and molecular immunology*, W.B. Saunders company, Philadelphia, 1997, pp. 285–286.
- [56] M.C. Subauste, D.C. Choi, D. Proud, Transient exposure of human bronchial epithelial cells to cytokines leads to persistent increased expression of ICAM-1, *Inflammation* 25 (2001) 373–380.
- [57] G. Richard, Connexins: a connection with the skin, *Exp. Dermatol.* 9 (2000) 77–96.
- [58] W.H. Evans, P.E. Martin, Gap junctions: structure and function (Review), *Mol. Membr. Biol.* 19 (2002) 121–136.
- [59] M. Kretz, K. Maass, K. Willecke, Expression and function of connexins in the epidermis, analyzed with transgenic mouse mutants, *Eur. J. Cell. Biol.* 83 (2004) 647–654.
- [60] V.A. Krutovskikh, C. Piccoli, H. Yamasaki, Gap junction intercellular communication propagates cell death in cancerous cells, *Oncogene* 21 (2002) 1989–1999.
- [61] N.K. Haass, K.S.M. Smalley, M. Herlyn, The role of altered cell-cell communication in melanoma progression, *J. Mol. Histol.* 35 (2004) 309–318.
- [62] K.K. Wilgenbus, C.J. Kirkpatrick, R. Knuechel, K. Willecke, O. Traub, Expression of Cx26, Cx32 and Cx43 gap junction proteins in normal and neoplastic human tissues, *Int. J. Cancer.* 51 (1992) 522–529.
- [63] J. Tada, K. Hashimoto, Ultrastructural localization of gap junctional protein connexin 43 in normal human skin, basal cell carcinoma and squamous cell carcinoma, *J. Cut. Pathol.* 24 (1997) 628–635.
- [64] P. Coutinho, C. Qiu, S. Frank, K. Tamber, D. Becker, Dynamic changes in connexin expression correlate with key events in the wound healing process, *Cell. Biol. Int.* 27 (2003) 525–541.
- [65] P.I. Jara, M.P. Boric, J.C. Saez, Leukocytes express connexin 43 after activation with lipopolysaccharide and appear to form gap junctions with endothelial cells after ischemia-reperfusion, *Proc. Natl. Acad. Sci. USA.* 92 (1995) 7011–7015.
- [66] T. Nagira, S.B. Matthew, Y. Yamakoshi, T. Tsuchiya, Enhancement of gap junctional intercellular communication of normal human dermal fibroblasts cultured on polystyrene dishes grafted with poly-N-isopropylacrylamide, *Tissue. Eng.* 11 (2005) 1392–1397.
- [67] E.J. Hall, The bystander effect, *Health. Phys.* 85 (2003) 31–35.